Sedimentology (1976) **23**, 87–105

Measurements of density underflows from Walensee, Switzerland*

ANDRÉ M. LAMBERT, KERRY R. KELTS *and* NEIL F. MARSHALL†

Geological Institute, ETH, Zurich, Switzerland and †*Scripps Institution of Oceanography, University of California, La Jolla, U.S.A.*

ABSTRACT

Speed and direction of bottom currents induced by density underflow of two sediment-laden rivers were measured by oceanographic current meters in the Walensee (= Lake of Walenstadt), Switzerland. The apparently shooting flow of currents (up to 30 cm/s in this study) is suggested as an explanation for laminations in turbidite sequences. The current speed apparently stabilizes on slopes around 2°; this angle seems to correspond to the critical slope where the flow of the measured currents becomes steady. Current direction is controlled by bottom topography and direction of river inflow. Reversal of current direction observed at two sites is probably due to the underflow-induced backward motion of the overlying lake water. Underflow activity in Walensee is correlative with density peaks of the river water input. The currents are compared to Lake Mead (Southwestern U.S.) underflows and sporadic currents in some submarine canyons.

INTRODUCTION

Density current phenomena have been described in a flurry of papers since the Grand Banks event was interpreted in 1952 as causing a turbidity current (Heezen & Ewing, 1952). Walker (1973) reviewed the progress of research on turbidity currents and their deposits. A generally applicable and geologically useful quantitative theory has yet to be presented. In order to confine the theory, many more critical observations, especially direct measurements, will be necessary. The problem of studying recent marine turbidity currents is that they are difficult to localize. Experiments in the laboratory have been very useful (Middleton, 1966a, b; Hand, 1974) but it is often quite problematic trying to apply the experimental results to nature. Despite many

* Contribution No. 74 of the Laboratory of Experimental Geology, Swiss Federal Institute of Technology, Zurich, Switzerland.

limitations, studying density currents in lakes has proven to be a very useful 'middle-ground compromise'.

The precedent for those studies goes back to the classic work done by Alphonse Forel (1889–96). He attributed the origin of channels and levees in the Rhone-delta cone of Lake Geneva to the underflow of cold, sediment-laden alpine meltwater. Gould (1960) described density underflows in Lake Mead; those currents travelled several tens of kilometres, and average velocities have been calculated as 15 cm/s (Bell, 1942).

A research project to study Swiss Lakes was initiated in 1967 by the Swiss Federal Institute of Technology in cooperation with the University of Bern. Our activities include piston coring, seismic profiling, current and heatflow measurements.

Piston core analysis showed that graded sand layers with turbidite character are a common occurrence in most of the investigated lakes (e.g. Sturm & Matter, 1970; Kelts & Briegel, 1971; Thompson & Kelts, 1974). These layers are considered to be the deposits of turbidity underflows which apparently occur in some Swiss lakes during high water periods. In order to better define the nature of such underflows our limnogeology group initiated a pilot study in cooperation with F. P. Shepard from the Scripps Institution of Oceanography to directly measure these bottom currents. We intend to obtain numerical information on the velocity and thickness of turbidity underflows. This paper primarily presents the results of our measurements from the Walensee (= Lake of Walenstadt).

CURRENT MEASUREMENTS

An intensive 3-week campaign (twenty-two stations) was planned for measurements in the perialpine lakes of Lucerne, Brienz, Zurich, and Walenstadt. These all have important tributaries which might induce sediment underflows. Timing was arranged to correspond with the spring melting season in the Alps, when the rivers were expected to be swollen with cold, sediment-laden waters. However, it was probably a happy coincidence in timing with heavy rainfalls which made possible the most significant results in the Walensee. This was the only lake investigated, confirming the existence of bottom currents with velocity peaks of up to 30 cm/s capable of eroding sediment. The data from the other lakes were less satisfactory. Currents were found in all lakes, but the generation of weaker water motions may be attributed to factors other than density differences, such as thermal overturn, wind, seiches, coriolis forces, etc. Only the strong bottom currents of the Walensee could be definitely interpreted as density underflows.

INSTRUMENTATION

The current meters used are of the Isaacs-Schick-Savonius rotor-type (Isaacs *et al.*, 1966; Shepard & Marshall, 1973a). The devices were vertically suspended between a weight on the lake floor and glass floats (see Fig. 1). The current meters were released from the anchoring weight after a preset timer activated an explosive bolt. The releases functioned properly on all twenty-two stations.

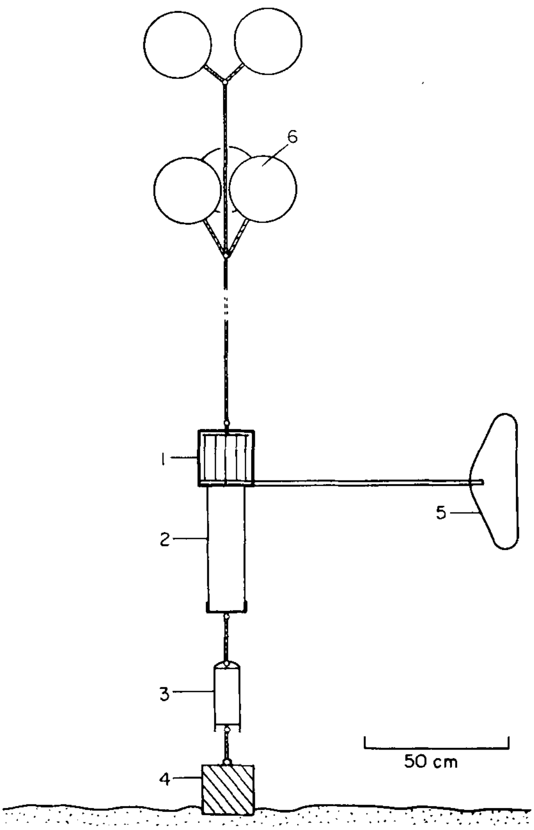

Fig. 1. Configuration of Scripps current meter (Isaacs-Schick-type) on the lake floor. 1, Housing with Savonius rotor; 2, electronic recording and compass packages; 3, automatic release; 4, concrete weight; 5, direction sensor van; 6, glass floats.

The meters are auto-recording: current speed and direction are registered on a pressure sensitive paper tape (see for example Fig. 10). The current direction is indicated by the position of a line on the paper, whereas the speed has to be calculated from the number of tick marks per time unit. One tick corresponds to a preset number of revolutions of the Savonius rotor. At one station (L–3) the current velocity could not be exactly determined because the setting used for this meter was too low and the ticks are spaced so closely that they form a solid line.

The data obtained from the lake measurements were analysed by computer at Scripps Institution of Oceanography. The type of graphs used to interpret the records represents a current vector analysis in which the velocity vector is plotted for two components (see for example Fig 12). The reader is referred to Shepard, Marshall & McLoughlin (1974a) for a more extended discussion of techniques.

RESULTS

The current measurements in the Walensee concentrated on the delta areas of two tributaries, the Murg Stream and, especially, the Linth River (see Figs 2, 3 and 7). The depth and recording time of the different stations is summarized in Table 1.

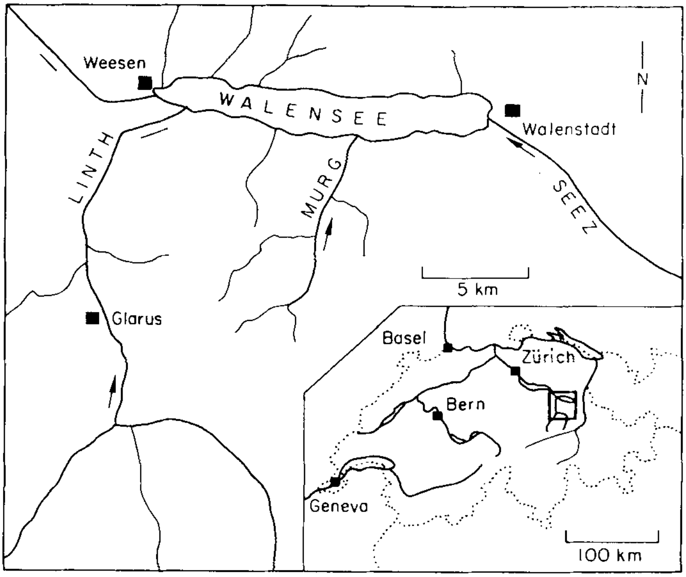

Fig. 2. Index map for the area of investigation: Lake of Walenstadt (= Walensee), Switzerland.

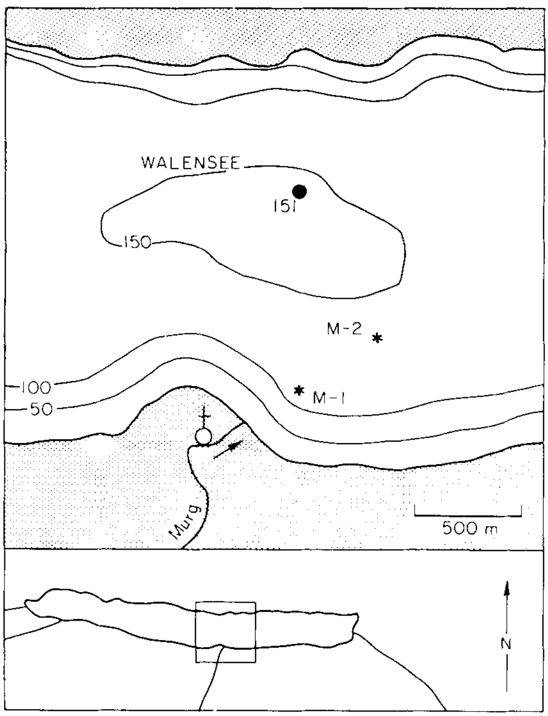

Fig. 3. Position of Stations M-1 and M-2 out from the Murg delta in the central part of the Walensee. Contour depth in metres.

Table 1. Depth and recording time of current meters

Station	Depth	Height of meter above bottom	Recording period	Start
M-1	115 m	1·5 m	21 h 00 min	7 May, 1973, 19 : 00
M-2	145 m	1·5 m	20 h 30 min	7 May, 1973, 19 : 00
L-1	100 m	1·5 m	63 h 50 min	4 May, 1973, 20 : 00
L-2	125 m	1·5 m	62 h 10 min	4 May, 1973, 20 : 15
L-3	90 m	1·5 m	62 h 35 min	4 May, 1973, 20 : 05
L-4	100 m	1·5 m	20 h 45 min	7 May, 1973, 20 : 00
L-5	131 m	8 m (L-5-2) 1·5 m (L-5-1)	193 h	21 May, 1973, 20 : 05

1. Murg Stream

Torrential floods in the Murg Valley, originating in the red Permian sandstones of the Glarus Alps, have built up a steep, cone-shaped delta, laterally adjacent to the deepest portion (151 m) of the lake. Layers of red sand, silt and clay ranging from several metres to a few mm thickness, were found in piston cores throughout the lake (Fig. 4). At the time of our field work, Murg stream was flowing at approximately one quarter capacity and the major surge of melt and rain water had already begun to subside when the stations (M–1 and M–2) were set. A plume of turbid water was still visible on the lake surface out to 100 m from the mouth, similar to the photograph shown in Fig. 9. Positions and depths of the two stations are summarized in Figs 3 and 4; the results in Fig. 5. The velocity reached a maximum of 5·4 cm/s during the first 3 h of measurement. This velocity peak appeared in station M–2, 2 h 20 min after its passage at station M–1 and seems to correlate as the same event.

The current meters were located 350 m from each other on a 2·5° slope. As it moved downslope, the current made a slight westward turn, heading toward the deepest part of the lake, thus conforming to the bottom topography. The westward deflection is expressed in the current direction analysis (Fig. 6, lowest graph).

2. Linth River

The Linth River also has its origin in the Glarus Alps but drains a greater area than the Murg stream. Sediments carried by the river comprise a mixture derived from Permian sandstones, Triassic to Cretaceous limestones, marls, and claystones, Tertiary Flysch sandstones, siltstones, and some crystalline material. The course of flow, in the lower reaches of the Linth River, was diverted into the Walensee by the construction of a canal, at the beginning of the 19th century. The Linth delta is the result of sedimentation since that time. A plume of turbid water forms during high water stages of the Linth (Fig. 9). In Table 2 some hydrometric data are compiled for the measuring period in the Linth area. Figs 7 and 8 show plan and cross-sectional views of the topography around the current meter stations occupied in the Linth river influx region.

Although not visible on the index maps, echograph and seismic recordings reveal the presence of numerous shallow furrows in the delta cone. A channel between 100 and 300 m wide, with a depth varying from 2 to 6 m, extends outwards about 1 km in alignment with the Linth Canal. It cuts the delta-foreset beds and culminates at the transition to the bottomset region. The slope of the foreset is about 20°.

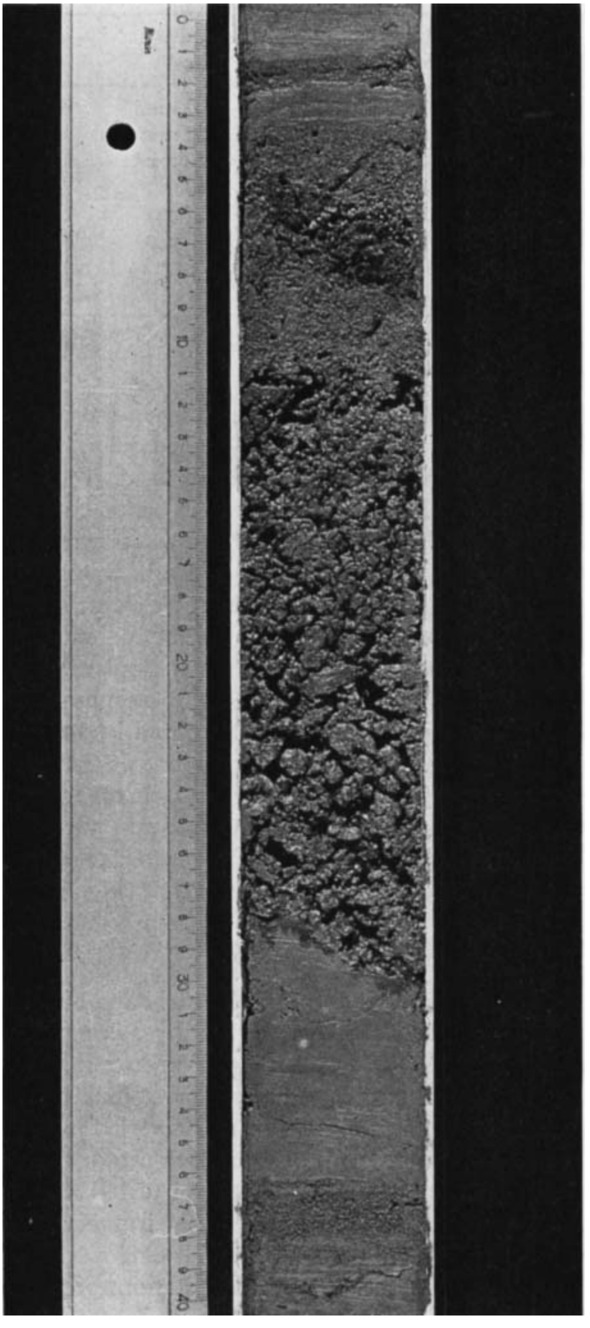

Fig. 4. Turbidite layer in a core from the central part of the Walensee, 4·85–4·50 m below the lake bottom. The maximum grain size is 10 mm.

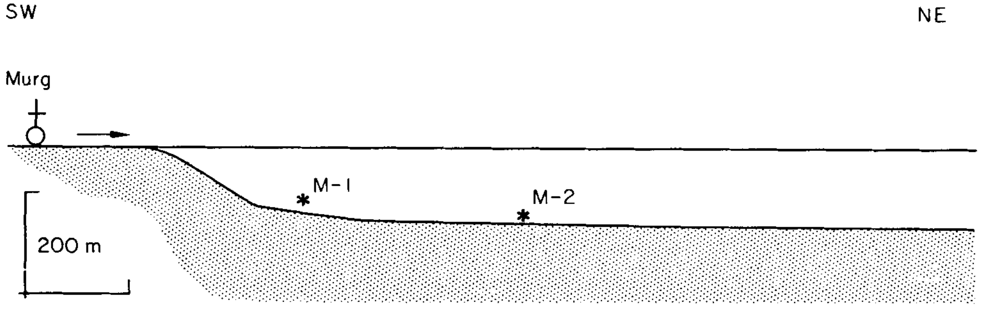

Fig. 5. Topographical cross-section through stations M-1 and M-2. No vertical exaggeration.

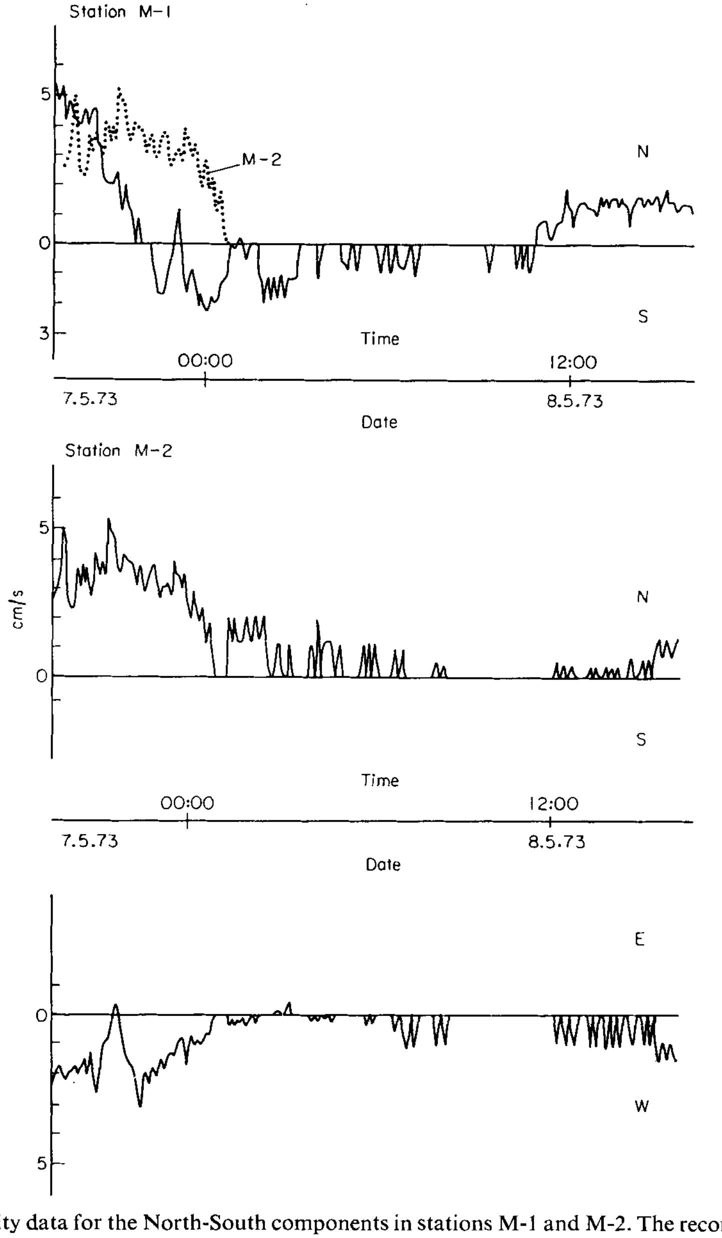

Fig. 6. Velocity data for the North-South components in stations M-1 and M-2. The record of station M-2 has been added in the uppermost diagram (dashed line) to demonstrate the time difference (2 h, 20 min) between the flow peaks (5·4 cm/s) in both current meters. An East-West component analysis (lowest graph) is added to illustrate the westward deflection of currents in station M-2.

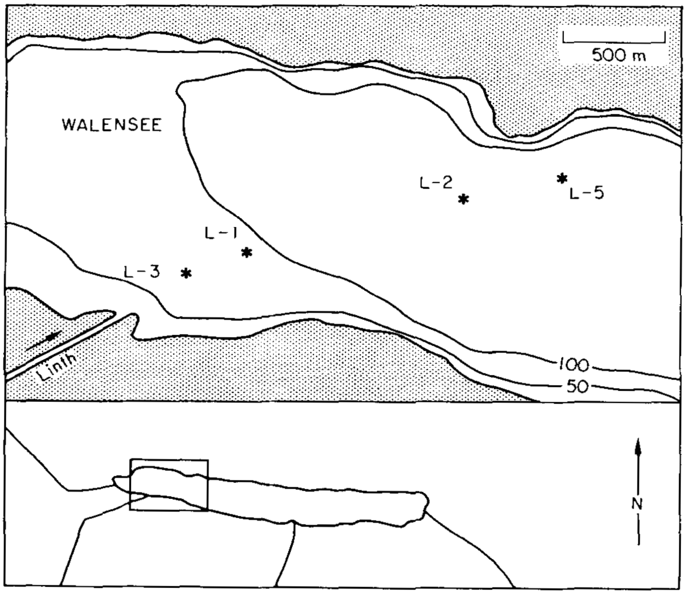

Fig. 7. Positions of stations L-1 through L-5 out from the Linth delta in the western part of the lakes. Station L-4 was placed 2 days later at the same position as station L-1. Contour depth in metres.

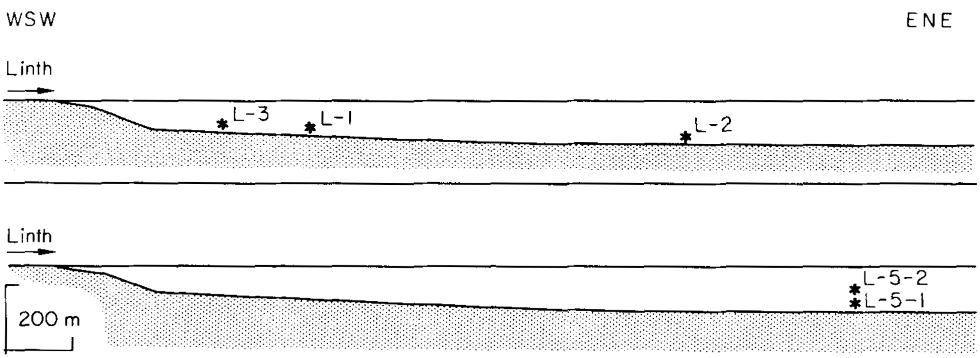

Fig. 8. Cross-section through stations L-1, L-2, and L-3 (upper part) and station L-5 (lower part). No vertical exaggeration. Slope angles: delta foreset 20°, bottomset 2°, lake floor 0°.

The measurements are summarized in Figs 10–13. First, the stations L–1, L–2, and L–3 were occupied to determine current velocity changes in the main channel axis. Then, after the presence of turbidity underflows was confirmed, station L–5 was occupied to gather information on the possible thickness of the currents.

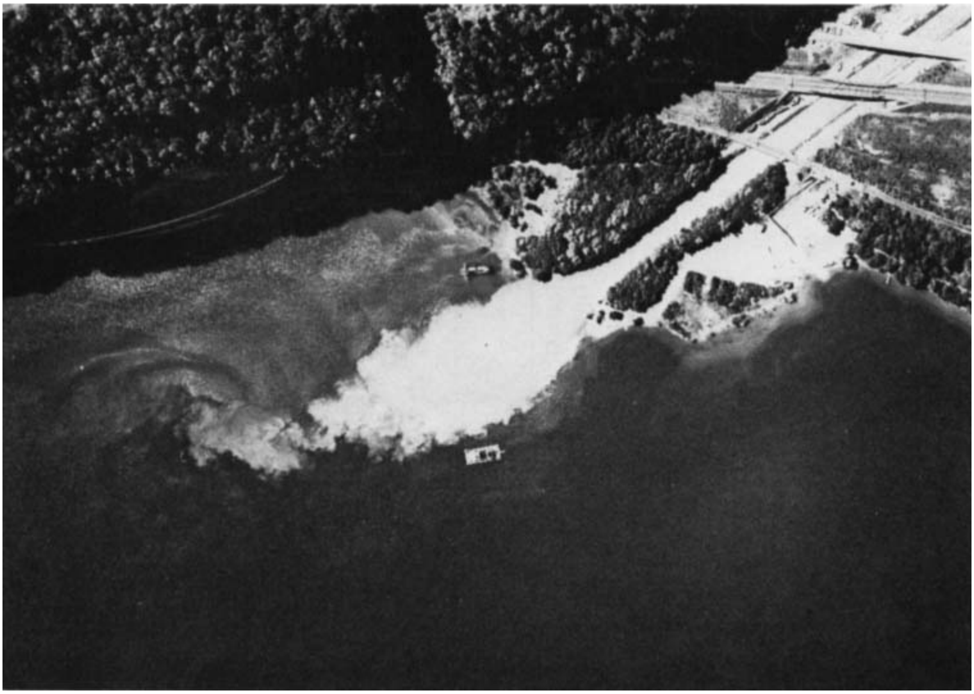

Fig. 9. Inflow of the sediment-laden Linth River into the Walensee forming a 'plume' of turbid water (9 June 1963). Courtesy of Swissair photo service.

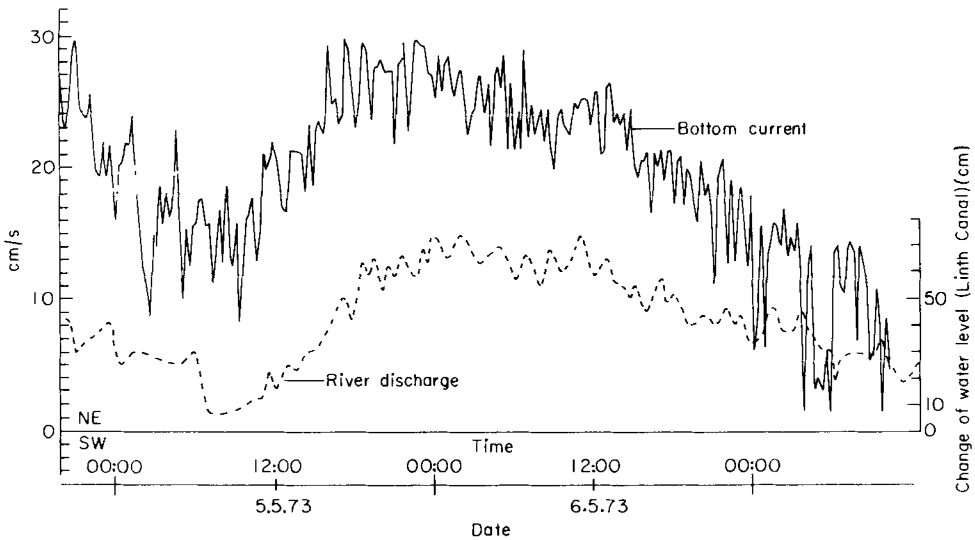

Fig. 10. NE-SW-components of current velocities recorded at station L-3 (solid line). The dashed line records the change of water level in the Linth Canal which is directly related to river flow volume and speed.

Table 2. *Hydrometric data of Linth River and Walensee, during the current measurements*

	Linth River					Walensee		
Station	Date May 1973	Discharge flow (m^3/s)	Suspended material (mg/l)	Temperature (°C)	Density (g/cm^3)	Temperature (°C)	Density (g/cm^3)	Density difference (g/cm^3)
L-1,2,3	4	78·8	564	6·8		8·5		
	5	91·0		7·2		8·9		
	6	108·0	1400	6·1	1·00134	7·4	0·99990	0·00144
	7	86·2		6·3		6·8		
L-4	8	69·8	386	5·9	1·00034	7·6	0·99990	0·00044
	20	54·2		8·5		9·6		
L-5	21	61·0	195	7·7	1·00005	9·5	0·99980	0·00025
	22	61·0		8·2		9·6		
	23	61·0		8·2		8·7		
	24	57·5	139	8·4		8·5		

Station L-3

The highest current velocity measurements (>30 cm/s) obtained during our field campaign have been recorded at this station (Fig. 10). The velocity fluctuates, and this pulsating pattern is obvious on the original current meter record (Fig. 11). Other evidence for the passage of strong currents was the presence of coarse sand found between the rotor and housing of the current meter after the recovery. The sand was deposited from a fast current as it flowed past the meter. This deposited sand may, in fact, have slightly hindered the motion of the rotor, and thus led to an underestimate of current strength.

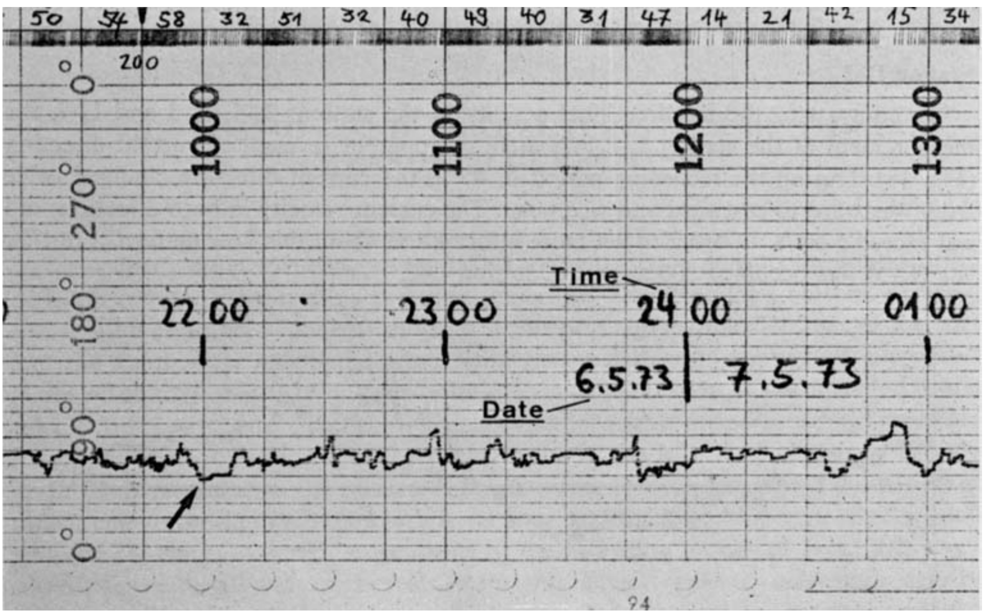

Fig. 11. Part of the original record obtained from station L-3 (Linth delta). Speed is determined by number of ticks per time interval (top of record). Note the periodic 'bunching' of ticks indicating pulsing flow character. Direction of flow is given by the position of the solid line (arrow) on the paper tape. Note the typical current caused oscillations.

Stations L–1 and L–4

The station L–1 did not provide any direct velocity data because the Savonius rotor remained locked throughout the recording period. However, an estimate can be obtained by looking at the direction record (Fig. 12). Cavitation along the direction-sensor van causes irregular, high frequency, low amplitude oscillations visible on the records. The presence of strong currents comparable to those from station L–3 is suggested by the similarity in the characteristic pattern of the direction records and further by the presence of coarse sand and vegetation debris on the housing and rotor. This site was reoccupied 3 days later by station L–4; the meter then recorded speeds up to 12 cm/s but the period of heavy rainfall was over and stream inflow had decreased substantially.

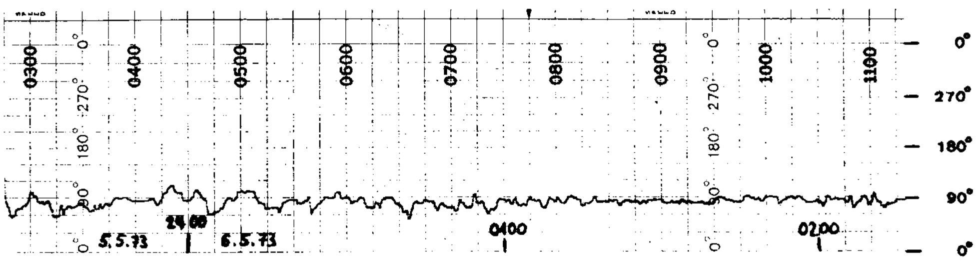

Fig. 12. Part of record obtained from station L-1 (Linth delta). No current speed ticks appear, due to a locked rotor. However, the oscillations of the direction record might suggest similar velocities to those recorded at station L-3.

Station L–2

In contrast to the unidirectional activity in the stations L–1, L–3 and L–4, the measurement at the station L–2 indicated an apparent reversal of current direction (Fig. 13). During the recording period of 45 h, the current direction changed twice from westward to eastward and *vice versa*. The current velocity in both directions did not exceed 5 cm/s. In order to get more information about this flow pattern, a further site (L–5) was occupied 500 m east of station L–2.

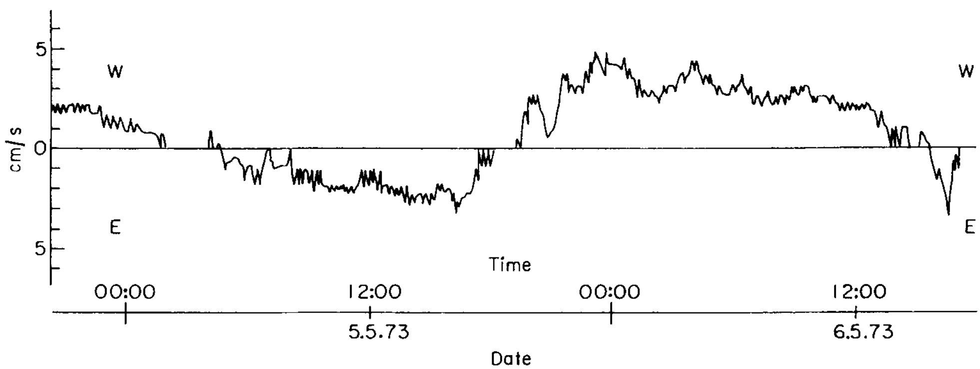

Fig. 13. E-W-components of the current velocities recorded at station L-2.

Station L–5

At this station (see Table 2 and Figs 6 and 7 for positioning) two meters were suspended one above the other with a vertical separation of 6 m, the lower meter 1·5 m above bottom. The recordings (Fig. 14) from the lower meter (L-5-1) are comparable to the results from station L–2. The current direction was initially westward at a speed of 3 cm/s. Then follows a period of 15 h of eastward current activity with a speed maximum of 6 cm/s. Finally the direction measured by the lower meter was again westward.

The upper meter (L–5–2) showed no activity during the westward current periods in the lower meter but it precisely recorded a westward (300°) current while the direction in the lower meter was nearly opposite (85°).

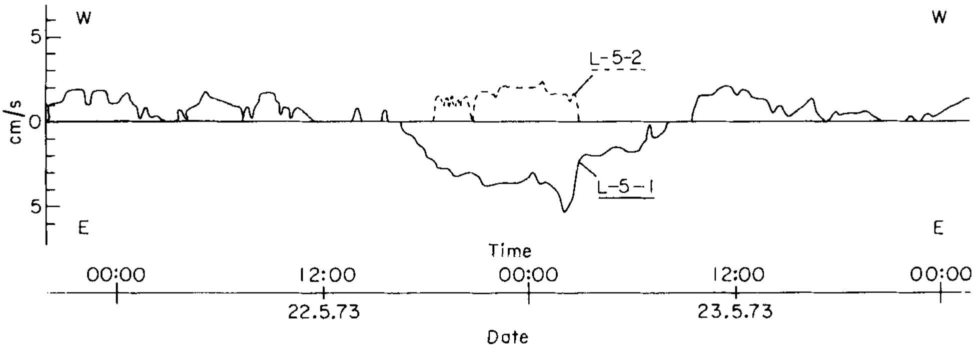

Fig. 14. E-W-components of the current velocities recorded at station L-5; the solid line from the lower meter (1·5 m above bottom) and the dashed line from the upper meter (8 m above bottom).

DISCUSSION AND CHARACTERISTICS OF THE MEASURED CURRENTS

Densities

The density difference between the lake and the tributary permits the continuation of Linth inflow to proceed as turbidity underflow along the lake bottom, carrying coarse sand and finer sediments out into its deepest region. The densities of the lake and the Linth were calculated from temperature data plus content of suspended matter (Table 2). Bed load or near bottom sediment transport is not included in the calculations but may be significant. The lake is thoroughly mixed in spring; therefore it seems a fair assumption that the deeper parts of the lake have similar or slightly lower temperatures than the surface. It is interesting to note that during the period of measurements in May 1973 the Linth River was carrying up to 1400 mg/l of suspended material (Table 2). After thunderstorms in the following month of July, 3026 mg/l suspended material was registered. From this annual peak a maximum density difference of 0·0416 g/cm^3 arises considering water temperatures for the river and lake of 9·5°C and 17·7°C respectively.

Direction of flow

Propagation directions of the underflows in the Walensee are controlled primarily by the direction of the inflow and by the bottom topography. This is clearly indicated by the eastward deflection of the north-east trending currents from the Linth River. The current vectors remain roughly perpendicular to the bathymetric contours. Similarly, currents from the Murg inflow are deflected to the west towards the deepest portion of the lake along slope gradients of about 2·5°. No distinct channels are known from the Murg delta. In the Linth delta the direction of the underflow is parallel to the channel axis.

A problem arises concerning the change of current to the nearly opposite direction observed at stations L–2 and L–5. It should be recalled that both stations were on the same flat part of the lake (Fig. 7). However, they recorded current activity at different times; L–2 as a single station 1·5 m above bottom and L–5 stacked with one meter at 1·5 m and the other 8 m from the bottom. Either there had been two sets of bottom currents, or we were recording a variation in current thickness. Consideration of the conservation of mass demands that for each density underflow there must be a consequent returnflow of the overlaying water. One interpretation of the current pattern at station L–5 is that the Linth underflow is responsible for the eastward currents, whereas the westward currents are due to the consequent returnflow of the lake water. The underflow would then have variations in its thickness: in one case the lower meter (L–5–1) recorded only the returnflow (Fig. 14); this means that the underflow thickness could not exceed about 1 m. In the other case the underflow was recorded in the lower meter, its backflow in the upper one. Therefore the thickness of the underflow at this time must have been on the order of 7 m considering that the upper meter was placed 8 m above bottom.

We note that the main directions of the underflow and its returnflow are not exactly opposite but about 40° discordant. The direction of the returnflow might be influenced by other factors, such as thermal or wind-induced overturn, etc. An alternative explanation, which would account for this discordance, would be the interaction of two underflows with a different density and origin. The denser underflow—of the Linth in our case—would displace upward a less dense westward underflow (Fig. 15). This longitudinal density current could have its origin at the eastern end of the Walensee (Fig. 2), where a discharge flow peak of 28·9 m^3/s was registered in the Seez River, 2 days before our measurements at station L–2. The sediment load was about 700 mg/l. If an underflow of the Seez River reached station L–2, this would suggest a current continuity over 11 km and a travel time of about 50 h, assuming an average velocity of 6 cm/s.

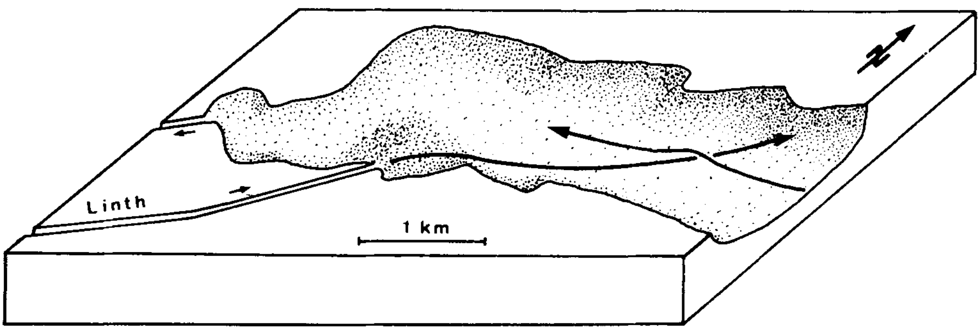

Fig. 15. Block diagram to illustrate a possible interaction of two currents recorded at station L-5, in which the Linth underflow displaces upward a basin-longitudinal current.

Current dimensions

An estimate of current width is difficult because we have no horizontal measurement profiles perpendicular to the flow direction. Limits are probably imposed by the width of the channels; 100–300 m in the Linth region.

We have fewer uncertainties concerning current thickness. If we accept the conclusion that the westward flow in the upper meter of station L–5 was the returnflow from the Linth underflow, this latter could not exceed 6 or 7 m thickness. This value is in good agreement with the Linth channel depth (6 m) but also seems to be a maximum value, because the returnflow was registered in the lower meter most of the time and thus could not exceed 1·5 m thickness. Kersey & Hsü (1975) estimate 10 m on a theoretical basis involving frictional energy loss and the critical slope angle θ_c.

Current velocities

Station L–3, where the highest velocities (30 cm/s) were recorded, was positioned 200 m from a site where a break in slope occurred; the change of slope angle is 18°. The rotor of this current meter was located about 1·5 m above bottom. Judged on basis of experimental results (Kersey & Hsü, 1975) the velocity may have been even greater nearer the bottom. The discharge flow of the Linth canal was registered by continuous monitoring of the water level 5 km up the river. The variations are clearly reflected in the current speed record (Fig. 10). At station L–3 the current speed fluctuated, but exceeded 18 cm/s during 26 h. Currents of such speed are capable of eroding and transporting sand (Hjulstrøm, 1939; Sundborg, 1956). The eroding power of the currents is also demonstrated by the presence of new, abandoned and filled channels discovered on echograms in the subaqueous delta off the Linth. The channels, 6 m deep, have been cut into sediments which include coarse gravel layers.

After the currents reach the flat bottom of the lake they have lost considerable momentum (compare stations L–3 and L–2). In the current measurements of the Murg underflow the time delay registered between the current speed peaks (5·4 cm/s in both current meters) is 2 h 20 min (Fig. 6). This is equivalent to the time that a current would need to travel 450 m (distance between the meters) with a constant velocity of 5·36 cm/s. This implies that there was no change in current speed between the two current meters although the slope is 2·5°. We conclude that the velocity of the Murg underflow tends to remain constant at about 5 cm/s on this slope, which may correspond to the critical angle θ_c (Kersey & Hsü, 1975) at which the frictional energy loss of a density current moving downslope is compensated by the available potential energy. Currents initiated by the Linth River sustain speeds of 6 cm/s 2·5 km from the origin (Fig. 7). How much farther they retain a discrete identity is a matter of conjecture. Nevertheless, the presence of numerous 1–5 cm thick graded silt layers in piston cores taken from the Linth delta to the center of the lake suggests travel distance ranging up to at least 10 km.

Pulsating flow

A remarkable observation can be made from the flow character registered in station L–3 (Figs 10 and 11). The relatively high-velocity currents are not steady, but rather the record shows a series of irregular pulses with a rough periodicity of 15–20 min. These pulses are not symmetric, as first there is a slight and then a rapid increase of the current to the peak velocity. Its decay is 'exponential' and less rapid than the build-up. A second pulse then follows, sometimes before the first has entirely subsided. The pulsating nature of the current at station L–3 may be due to its supercritical velocity and therefore shooting flow (Massey, 1968, p. 333). The ratio

$$\frac{u}{\sqrt{g \cdot \dfrac{\Delta\rho}{\rho} \cdot h}} = (\mathrm{Fr}) \quad \text{(Densiometric Froude number)} \qquad (1)$$

where u is the current velocity, h the current thickness' $\Delta \rho$ the effective density, ρ the density of the lake water, and g the gravitational constant, defines the character of flow. The critical velocity is given by

$$u = \sqrt{g \cdot \frac{\Delta\rho}{\rho} \cdot h} \qquad \text{or (Fr)} = 1. \tag{2}$$

Flow in which (Fr) < 1 is called tranquil; when (Fr) > 1, flow becomes rapid or shooting.

Using Eq. (1) we can calculate a densiometric Froude number of about 1·3 for the underflow at station L–3 (u = 30 cm/s, $\Delta\rho$ = 0·001 g/cm^3, ρ = 1 g/cm^3, $h = 5 \times 10^2$ cm). Therefore we can expect a shooting flow, although we used a maximum value of 5·0 m for the current thickness h; for smaller values the Froude number would increase. Hand (1974) based on his flume experiments, also postulates that supercritical conditions are common in turbidity flows. Walker (1973) noted that one of the unsolved problems of turbidite deposits was the lack of an explanation for the upperset laminations commonly encountered. Short period pulsations in the body-speed of a depositing current could easily lead to the structures observed.

Another explanation for the pulsating nature of the currents would be that the river inflow is not steady. However, the water level monitors in the canal did not show periodic changes which correlate with the frequencies observed in the current meter records.

COMPARISON WITH LAKE MEAD

Interesting parallels concerning underflow activity are observed comparing results of Walensee and Lake Mead. Current speed data cited in Gould (1960) are not reported from direct measurements, rather they represent average values calculated from the time delay between the observation of underflows in the Colorado River inlet area and the subsequent arrival at Hoover dam. The frequency of underflows was reported as twelve flows within 7 years; in Walensee we might expect up to four comparable underflows per year depending on high water stages of the Linth. As in Walensee, Lake Mead underflows correlate with density maxima in the river inflow, (up to 1·02 g/cm^3), and the average velocities are on the order of 10–20 cm/s with maxima of 30 cm/s near the delta front (cf. Bell, 1942). In the flatter parts of the lake, current speeds were generally around 7 cm/s. Lake Mead currents were able to sustain flow momentum although the slope was only about 0·1°, which would therefore be equivalent to the critical angle θ_c (Kersey & Hsü, 1975).

COMPARISON WITH SUBMARINE CANYONS

A comparison of our results with measurements of density currents in submarine canyons associated with major rivers is hampered by the scarcity of data from such areas. Shepard & Emery (1973) measured bottom currents in the Congo Submarine Canyon where surprisingly they found the currents to be predominantly upcanyon. This was interpreted to be due to fresh water overflow which draws bottom waters upwards.

An interesting parallel is offered by the current meter measurements in the submarine canyon of the Var River in the French Riviera (Gennesseaux, Guibout & Lacombe, 1971). The current meter was placed 1·5 m above bottom, similar to the stations in Walensee. Current speed peaks of 86 and 119 cm/s were recorded during storm conditions. The authors conclude that the main cause for these strong currents were turbidity surges due to a rapid increase of the discharge flow in the Var River during heavy rainfalls. The flow pattern also seems to be pulsating. As the slope angle is about 6° the flow velocity should have been supercritical and the flow therefore shooting.

The cause of bottom currents in submarine canyons not, or no longer, associated with river inlet is discussed by Daly (1936), Shepard & Marshall (1973a) and Shepard *et al.* (1974a). The maximum current speeds commonly recorded in these canyons are of the same order as the peak flow speeds registered in Walensee or Lake Mead. However, there are important genetic differences. The canyon currents show directions both up and down the canyon axis correlating with tidal cycles (Shepard, Marshall & McLoughlin, 1974b). The authors conclude that most canyon currents therefore are due to internal waves rather than density controlled mass movement. Including the Var Canyon measurement only a few cases of down canyon currents stronger than those from lakes have been reported. In Scripps Canyon, Inman (1970) and others estimated currents up to 160 cm/s, and Shepard & Marshall (1973b) measured speeds up to 50 cm/s before the meter was swept away down canyon. These were in conjunction with heavy storm activity and may be analogous to the periodic highwater stages in the lakes. In Hydrographer Canyon speeds attained up to 50 cm/s (Shepard, personal communication). Keller *et al.* (1973) recognized a net down canyon transport of fine material in the Hudson Canyon, but measured average current speeds of only 8–15 cm/s with rare peaks up to 27 cm/s.

SUMMARY AND CONCLUSIONS

Current measurements in Walensee have confirmed the existence of periodic sediment-laden density underflows moving along the bottom of the lake towards its deepest region. These currents were induced by the sediment suspensions in the major tributaries and are probably responsible for graded sand and silt layers commonly encountered in the delta regions as well as in the distal lake sediments. Density contrasts with the surrounding lake water range from 0·00025 g/cm^3 to 0·04160 g/cm^3, limited by the density of the inflowing suspension. Direction of underflow motion is controlled by the direction of the river inlet and by the topography of the lake floor. The consequent returnflows, which have apparently been recorded at two stations do not show diametrically opposed directions as expected. A discordance of about 40° may be attributed to other factors, such as thermal or wind induced overturn. An alternative explanation suggests an interaction of two different underflows, the less dense current being discretely displaced upwards. Limits of current width are probably given by the channel which is 100–300 m wide in the Linth region. Current thickness probably varies with different slope angles. On slopes less than about 2°, 1·5–2 m seems to be the common thickness with maximums of about 5 m. The currents attain speeds of at least 30 cm/s on delta slopes greater than 2° and are thus capable of eroding and transporting coarse sand and finer sediments. The velocity appears to stabilize at about 6 cm/s on slopes of around 2° or less, which is apparently equivalent to the critical slope angle θ_c, where the available potential energy is compensated by frictional energy loss. A pulsating character seems to be typical for currents with high velocities, where the densiometric Froude number is >1 and the flow therefore shooting. This is a significant factor in the deposition of turbidite units. Density currents measured in the Walensee were comparable in physical parameters to those observed in Lake Mead and some submarine canyons.

We believe that there is good potential in applying the results of current measurements in lakes to the theoretical problems of density currents. Further studies will provide valuable data toward the understanding of processes in the oceans.

ACKNOWLEDGMENTS

We acknowledge the support of the Swiss Federal Institute of Technology and the Swiss National Research Foundation. The Swiss Federal Water agency in Bern kindly provided some hydrometric data. The study was also partially supported by the National Science Grant DES74–22089 and by the Office of Naval Research Grant N000 14–69–A–0200–6049. We thank Mr W. Bälly, game warden, for help during part of the field work. We would like to thank Dr K. Hsü and Dr F. P. Shepard who initiated discussions leading to this project and Dr D. Kersey for fruitful suggestions. They have also read early drafts of the manuscript.

REFERENCES

BELL, H.S. (1942) Density currents as agents for transporting sediments. *J. Geol.* **50,** 512–547.

DALY, R.A. (1936) Origin of submarine 'canyons'. *Am. J. Sci.* **31,** 401–420.

FOREL, F.A. (1892) *Le Léman,* **1,** 543 pp.

GENNESSEAUX, M., GUIBOUT, P. & LACOMBE, H. (1971) Enregistrement de courants de turbidité dans la vallée sous-marine du Var (Alpes-Maritimes). *C. r. hebd. séanc. Acad. Sci., Paris,* **273,** 2456–2459.

GOULD, H.R. (1960) Turbidity currents. In: *Comprehensive Survey of Sedimentation in Lake Mead, 1948–1949. Prof. Pap. U.S. geol. Surv.* **295,** 201–207.

HAND, B. (1974) Supercritical flow in turbidity currents. *J. sedim. Petrol.* **44,** 637–648.

HEEZEN, B.C. & EWING, M. (1952) Turbidity currents and submarine slumps, and the 1929 Grand Banks Earthquake. *Am. J. Sci.* **250,** 849–873.

HJULSTRØM, F. (1939) Transportation of detritus by moving water. In: *Recent Marine Sediments. Am. Ass. Petrol. Geol.* 5–31.

INMAN, D.L. (1970) Strong currents in submarine canyons. *Abstracts, Transactions of the American Geophysical Union,* **51,** 319.

ISAACS, J.D., REID, J.L., SCHICK, G.B. & SCHWARTZLOSE, R.A. (1966) Near bottom currents measured in 4 kilometers depth off Baja California coast. *J. geophys. Res.* **71,** 4297–4303.

KELLER, G.H., LAMBERT, D., ROWE, G. & STARESINIC, N. (1973) Bottom currents in the Hudson Canyon. *Science,* **180,** 181–183.

KELTS, K. & BRIEGEL, U. (1971) Sediment slides and turbidity current models from Swiss Lakes. Abstracts, *VIII International Sedimentological Congress,* p. 49.

KERSEY, D.G. & HSU, K.J. (1975) A physical approach to the flow of density currents (in preparation).

MASSEY, B.S. (1968) *Mechanics of Fluids,* 2nd edn, 508 pp. Van Nostrand Reinhold, New York.

MIDDLETON, G.V. (1966a) Experiements on density and turbidity currents. I. Motion of the head. *Can. J. Earth Sci.* **3,** 523–546.

MIDDLETON, G.V. (1966b) Experiements on density and turbidity currents. II. Uniform flow of density currents. *Can. J. Earth Sci.* **3**, 527–637.

SHEPARD, F.P. & EMERY, K.O. (1973) Congo Submarine Canyon and Fan Valley. *Am. Ass. Petrol. Geol.* **57**, 1679–1691.

SHEPARD, F.P. & MARSHALL, N.F. (1973a) Currents along floors of submarine canyons. *Am. Ass. Petrol. Geol.* **57**, 244–264.

SHEPARD, F.P. & MARSHALL, N.F. (1973b) Storm generated current in La Jolla Submarine Canyon, California. *Mar. Geol.* **15**, M-10–M-24.

SHEPARD, F.P., MARSHALL, N.F. & MCLOUGHLIN, P.A. (1974a) Currents in submarine canyons. *Deep Sea Res.* **21**, 691–706.

SHEPARD, F.P., MARSHALL, N.F. & MCLOUGHLIN, P.A. (1974b) 'Internal Waves' advancing along submarine canyons. *Science*, **183**, 195–198.

STURM, M. & MATTER, A. (1972) Sedimente und Sedimentations-Vorgänge im Thunersee. *Eclog. Helv.* **65**, 563–590.

SUNDBORG, A. (1956) The River Klarälven, a study in fluvial processes. *Geogra. Annlr*, **38**, 125–316.

THOMPSON, R. & KELTS, K.R. (1974) Holocene sediments and magnetic stratigraphy from Lakes Zug and Zurich, Switzerland. *Sedimentology*, **21**, 577–596.

WALKER, R.G. (1973) Mopping up the turbidite mess. In: *Evolving Concepts in Sedimentology* (Ed. by R. N. Ginsburg). *Studies in Geology*, **21**, 1–37. Johns Hopkins University Press.